Black Hole Universe

Multi-Mission and Wavelength Studies of Compact Binary Systems

ITN Back Hole Universe Meeting (09/22/2010 ~ 09/23/2010)

Yi-Jung Yang

Supervisor: Rudy Wijnands (API UvA)

Co-supervisors: Tom Maccarone (Southampton)

Jörn Wilms (FAU Erlangen-Nuremberg)

UNIVERSITY OF AMSTERDAM

Outline

- A very luminous Globular Cluster X-ray Source in M31
- Swift Observations of ULX Holmberg IX X-1
- Optical counterparts of ULXs in the BCD galaxy NGC4861
- Gamma-ray emission from PSR J1023+0038

Observation of Bo375 X-ray Source

Bo375 X-ray source was first discovered by Einstein High Resolution Imager (HRI) in 1979 during M31 survey observations. Later, it was also observed with ROSAT, ASCA, as well as many other on going X-ray satellites such as Chandra, XMM-Newton, Suzaku and Swift.

Di Stefano et al. (2002) conducted a Chandra survey of selected regions of M31, and found that the luminous source in their regions was associated with the globular cluster Bo375.

For more than 30 years, the source has been observed many times, and the luminosity has been found to be persistent all time (Lx > 4E38 ergs/s)

Possible explanations for the high luminosity

- the source might contain multiple components
- the source radiation might be beamed
- the source might be an accreting neutron star
- the source might be an accreting black hole

Observation Log of Bo375

Date	ObsId	Observatory	Instrument	Exposure	Remark
2000 – 11 – 01	2052	Chandra	ACIS-S	13.9 ks	Pile-up
2003 – 09 – 10	3813	Chandra	HRC-I	4.6 ks	
2004 – 11 – 25	4541	Chandra	ACIS-S	25.6 ks	Pile-up
2004 – 11 – 26	6167	Chandra	ACIS-S	24.2 ks	Pile-up
2006 – 07 – 08	0403530201	XMM-Newton	EPIC-PN	13.3 ks	Timing Mode
2006 – 07 – 10	0403530301	XMM-Newton	EPIC-PN	18.0 ks	Timing Mode
2006 – 07 – 12	0403530401	XMM-Newton	EPIC-PN	16.2 ks	Timing Mode
2006 – 07 – 14	0403530501	XMM-Newton	EPIC-PN	14.9 ks	Timing Mode
2006 – 07 – 16	0403530601	XMM-Newton	EPIC-PN	18.0 ks	Timing Mode
2007 – 01 – 02	0402561201	XMM-Newton	EPIC-PN	63.2 ks	Imaging Mode
2007 – 02 – 04	701028010	Suzaku	XIS0 XIS1 XIS3	12.8 ks	
2007 – 02 – 06	701028020	Suzaku	XIS0 XIS1 XIS3	15.5 ks	
2007 – 02 – 11	701028030	Suzaku	XIS0 XIS1 XIS3	12.5 ks	
2008 – 05 – 28	22001	Swift	XRT	3.4 ks	
2008 – 06 – 01	28001	Swift	XRT	2.8 ks	
2008 – 07 – 26	28003	Swift	XRT	4.9 ks	

A series of Chandra HRC-I 1.0 ks observations from 1999 to 2002 were also used to construct the long-term lightcurve of Bo375.

Radial Profile of Bo375 Chandra Observation

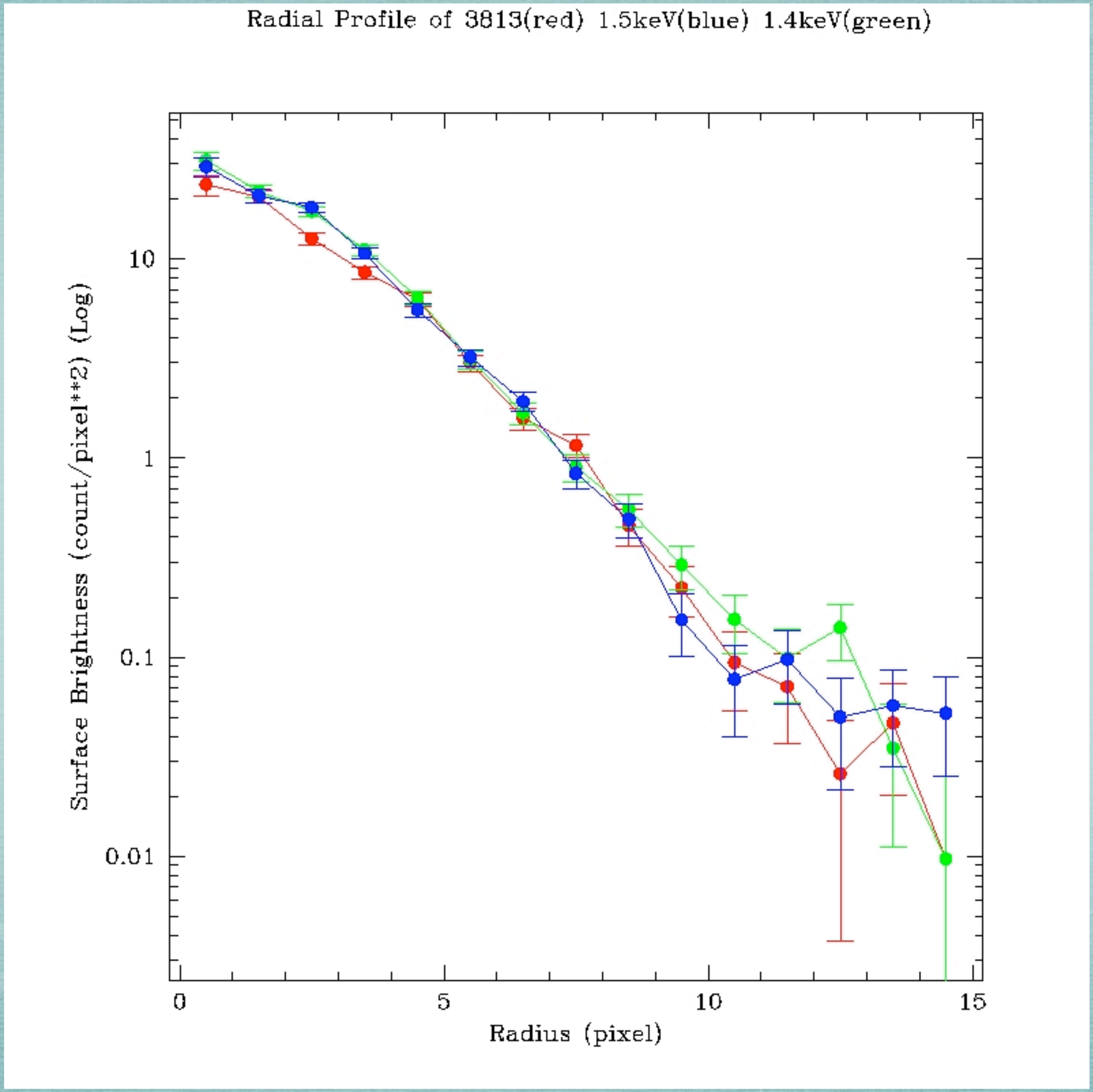

Example using M15

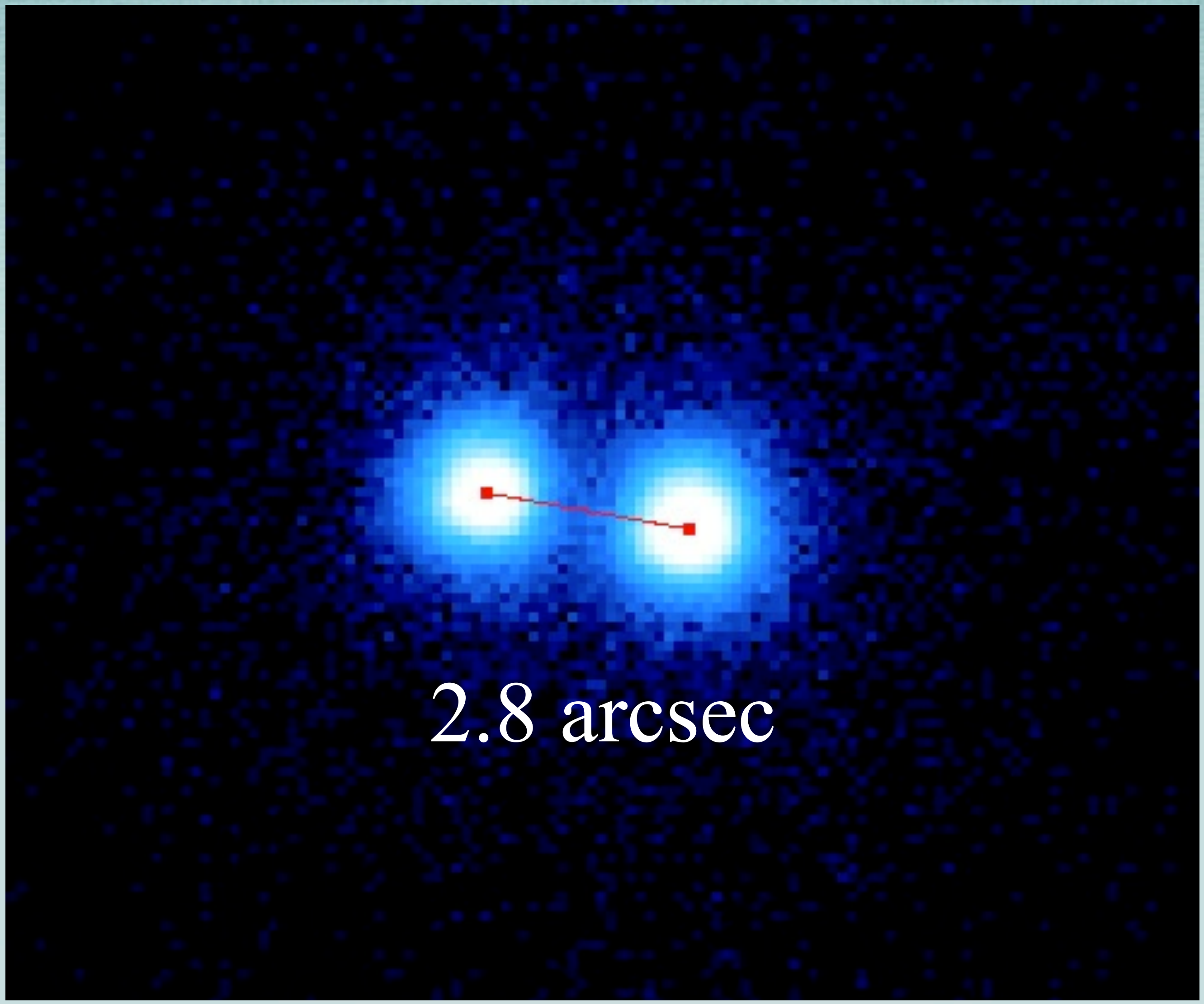

Assuming a distance of 9.98 kpc to M15, we can calculate the distance between these two sources. Apply the distance to Bo375 (distance to M31 is 780 kpc), the corresponding angular separation is 0.036”. Using 0.5” as Chandra limit for angular resolution, that gives ~2pc.

Short-term Lightcurve of Bo375

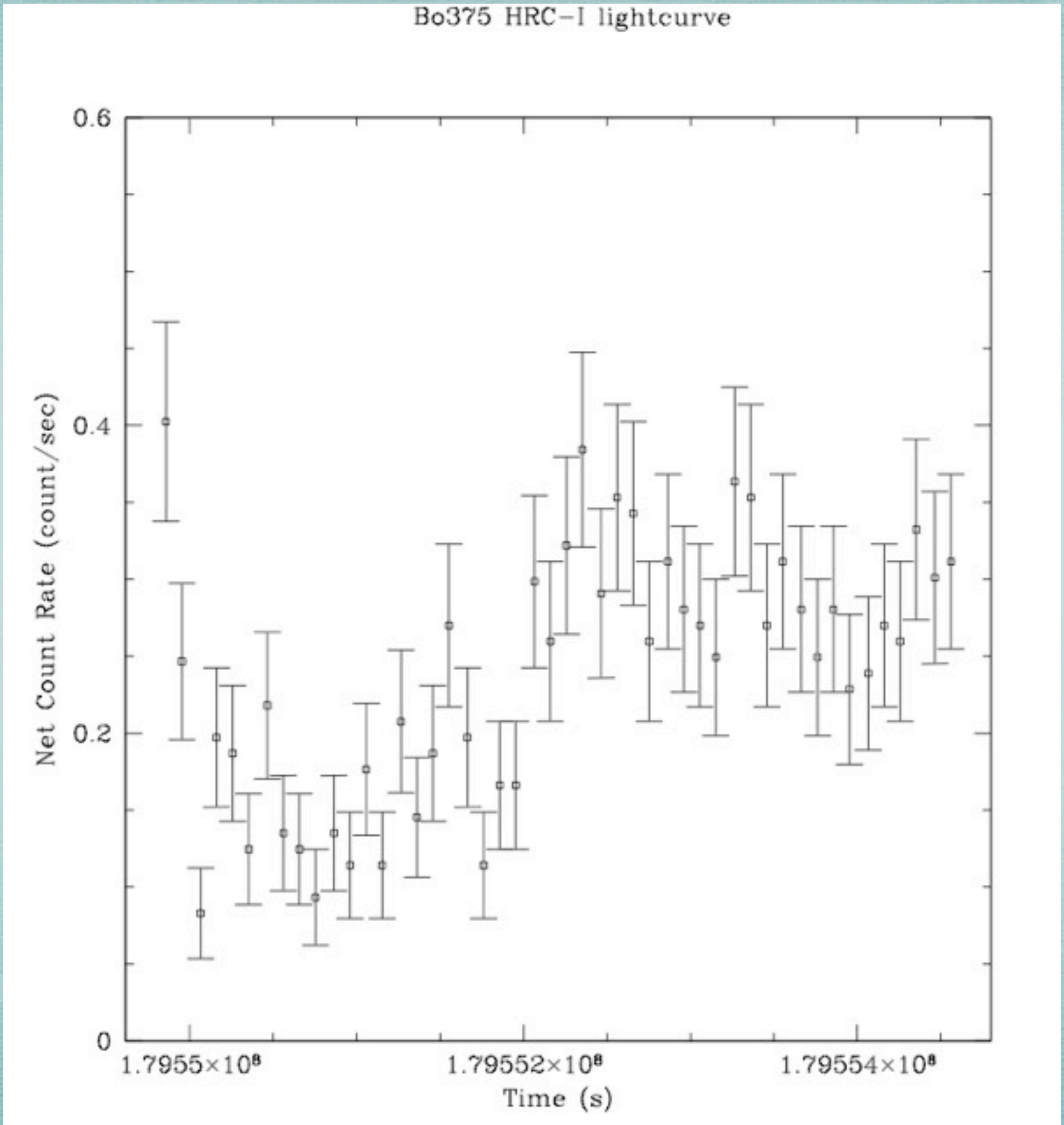

Multi-Mission Long-term Lightcurve

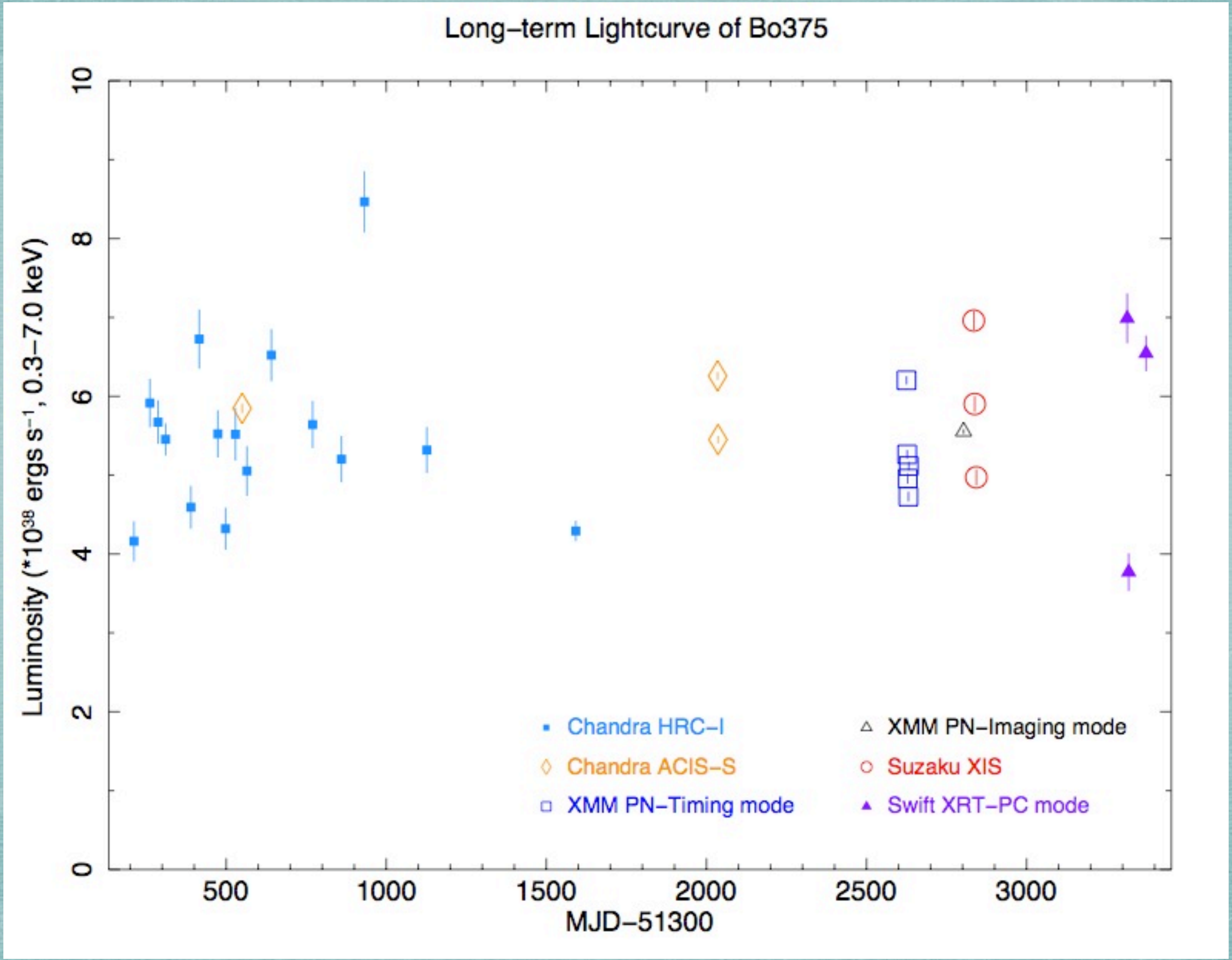

XMM-Newton Spectrum

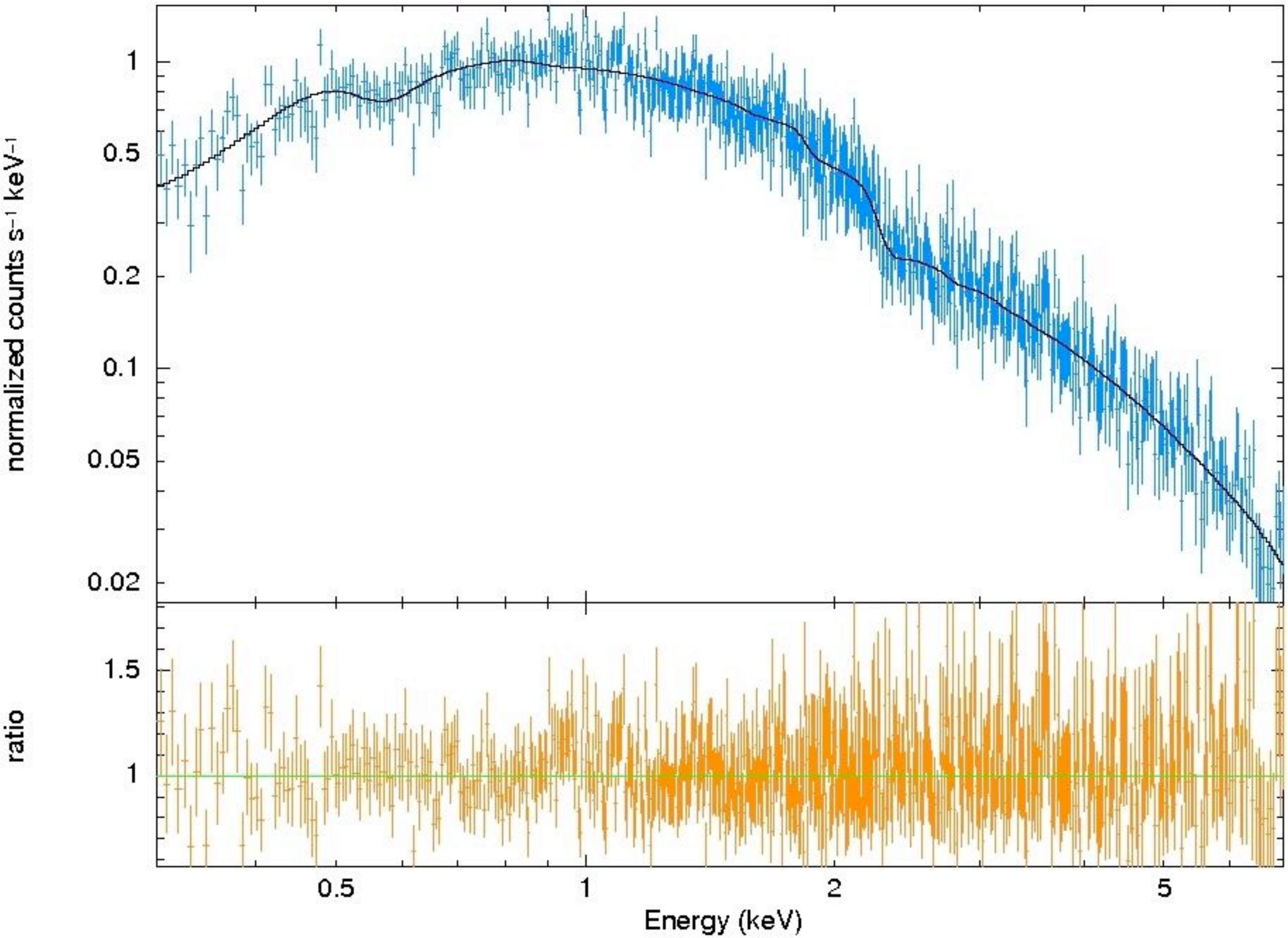

Suzaku Spectrum

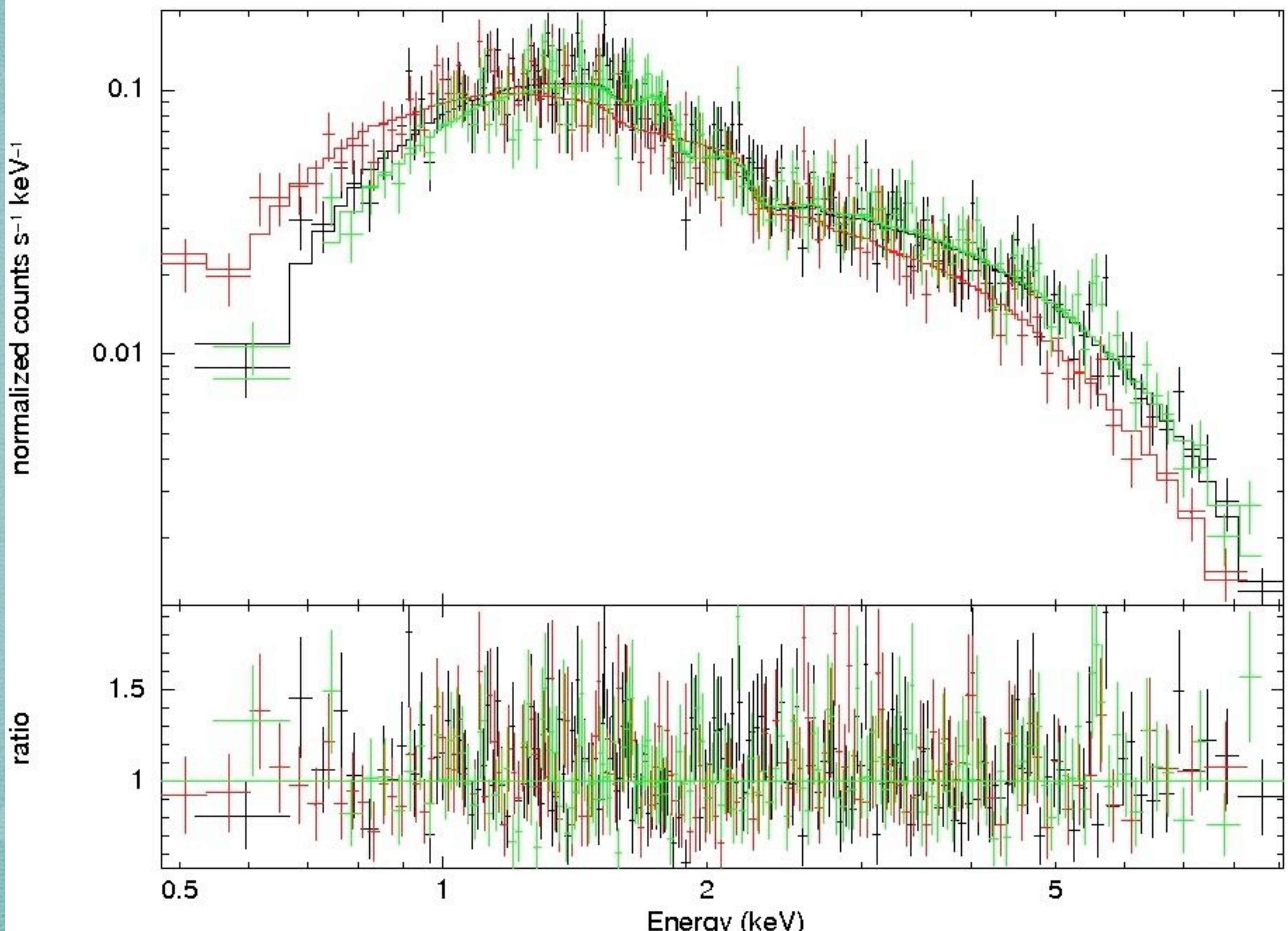

Power-Law + Blackbody Model

POWER-LAW + BLACKBODY

Observation	N_H^a	Γ	KT	χ^2/dof	F_X^b	F_{BB}^c	Ratio[d]	R_{EFF}^e
*xmm*0403530201	$5.2^{+1.7}_{-1.4}$	$1.95^{+0.13}_{-0.09}$	$0.90^{+0.06}_{-0.06}$	0.93/344	$10.6^{+0.2}_{-0.2}$	$2.6^{+0.3}_{-0.2}$	0.25	$47.2^{+5.4}_{-4.6}$
*xmm*0403530301	$5.1^{+1.7}_{-1.3}$	$1.85^{+0.12}_{-0.08}$	$0.96^{+0.07}_{-0.06}$	0.99/380	$9.3^{+0.2}_{-0.2}$	$2.1^{+0.3}_{-0.1}$	0.23	$37.2^{+5.1}_{-3.6}$
*xmm*0403530401	$3.5^{+1.5}_{-1.3}$	$1.74^{+0.08}_{-0.08}$	$0.95^{+0.11}_{-0.11}$	0.94/370	$9.1^{+0.2}_{-0.2}$	$1.4^{+0.3}_{-0.1}$	0.15	$31.3^{+6.4}_{-4.6}$
*xmm*0403530501	$3.2^{+1.5}_{-0.8}$	$1.77^{+0.06}_{-0.06}$	$0.94^{+0.10}_{-0.10}$	1.19/347	$8.9^{+0.2}_{-0.1}$	$1.6^{+0.3}_{-0.1}$	0.18	$33.8^{+6.2}_{-4.5}$
*xmm*0403530601	$3.0^{+1.4}_{-1.0}$	$1.75^{+0.09}_{-0.06}$	$0.90^{+0.06}_{-0.06}$	1.09/401	$9.0^{+0.2}_{-0.1}$	$2.1^{+0.1}_{-0.1}$	0.23	$41.5^{+4.1}_{-3.3}$
*xmm*0402561201(*PN*)	$5.8^{+0.9}_{-0.8}$	$1.93^{+0.08}_{-0.07}$	$1.05^{+0.06}_{-0.06}$	0.93/351	$8.4^{+0.1}_{-0.1}$	$1.8^{+0.3}_{-0.0}$	0.21	$29.2^{+3.1}_{-3.1}$
*xmm*0402561201(*MOS*)	$8.0^{+1.9}_{-2.4}$	$1.89^{+0.12}_{-0.13}$	$0.89^{+0.07}_{-0.09}$	1.03/212	$9.2^{+0.2}_{-0.2}$	$1.9^{+0.3}_{-0.2}$	0.21	$41.5^{+5.3}_{-5.6}$
*Suzaku*701028010	$6.7^{+4.1}_{-4.5}$	$1.87^{+0.16}_{-0.15}$	$0.89^{+0.09}_{-0.08}$	0.96/449	$10.7^{+0.6}_{-0.6}$	$2.8^{+0.2}_{-0.1}$	0.26	$52.0^{+6.4}_{-5.5}$
*Suzaku*701028020	$6.2^{+4.9}_{-3.9}$	$1.89^{+0.13}_{-0.15}$	$0.95^{+0.09}_{-0.08}$	0.91/464	$9.0^{+0.6}_{-0.4}$	$2.5^{+0.2}_{-0.0}$	0.28	$43.7^{+5.7}_{-4.2}$
*Suzaku*701028030	<8.4	$1.63^{+0.14}_{-0.12}$	$0.87^{+0.26}_{-0.17}$	0.82/331	$8.1^{+0.4}_{-0.2}$	$0.9^{+0.1}_{-0.0}$	0.11	$31.4^{+8.9}_{-8.1}$
*Swift*28003	$10.8^{+31.4}_{-10.8}$	$2.14^{+2.30}_{-0.53}$	$0.86^{+0.14}_{-0.14}$	1.13/33	$9.3^{+2.9}_{-1.5}$	$4.6^{+2.2}_{-2.4}$	0.49	$69.4^{+18.3}_{-20.8}$

Power-Law + Disk Blackbody Model

POWER-LAW + DISK BLACKBODY

Observation	N_H^a	Γ	T_{in}	χ^2/dof	F_X^b	F_{DISK}^c	Ratio[d]	R_{EFF}^e
*xmm*0403530201	$4.1^{+4.4}_{-3.1}$	$2.27^{+0.53}_{-0.41}$	$1.66^{+0.08}_{-0.15}$	0.93/344	$10.2^{+1.2}_{-0.5}$	$6.4^{+0.8}_{-0.8}$	0.63	$15.8^{+1.7}_{-1.3}$
*xmm*0403530301	$2.8^{+3.7}_{-2.5}$	$2.00^{+0.47}_{-0.32}$	$1.77^{+0.12}_{-0.20}$	0.98/380	$8.8^{+0.6}_{-0.3}$	$5.2^{+0.9}_{-0.5}$	0.59	$12.6^{+2.2}_{-1.2}$
*xmm*0403530401	$1.7^{+2.9}_{-1.7}$	$1.77^{+0.37}_{-0.21}$	$1.80^{+0.28}_{-0.36}$	0.93/370	$8.7^{+0.4}_{-0.2}$	$3.6^{+1.3}_{-0.5}$	0.41	$10.2^{+4.2}_{-1.5}$
*xmm*0403530501	$0.6^{+2.4}_{-0.6}$	~~$1.76^{+0.30}_{-0.15}$~~	$1.70^{+0.23}_{-0.19}$	1.16/347	$8.4^{+0.3}_{-0.1}$	$3.9^{+0.7}_{-0.2}$	0.46	$11.6^{+2.4}_{-1.8}$
*xmm*0403530601	< 2.4	$1.77^{+0.36}_{-0.14}$	$1.68^{+0.15}_{-0.11}$	1.07/401	$8.4^{+0.3}_{-0.0}$	$5.1^{+0.2}_{-0.5}$	0.61	$13.7^{+1.1}_{-1.6}$
*xmm*0402561201(*PN*)	$4.8^{+2.4}_{-1.9}$	$2.14^{+0.30}_{-0.24}$	$1.95^{+0.09}_{-0.14}$	0.94/351	$8.2^{+0.4}_{-0.3}$	$4.4^{+0.5}_{-0.6}$	0.54	$9.6^{+1.0}_{-0.6}$
*xmm*0402561201(*MOX*)	$5.9^{+0.6}_{-0.4}$	$3.40^{+1.6}_{-0.7}$	$1.64^{+0.12}_{-0.23}$	1.00/212	$8.6^{+0.1}_{-0.0}$	$5.0^{+0.2}_{-0.0}$	0.58	$14.4^{+3.4}_{-1.5}$
*Suzaku*701028010	< 5.8	$1.61^{+0.57}_{-0.23}$	$1.50^{+0.21}_{-0.15}$	0.96/449	$9.5^{+0.7}_{-0.0}$	$6.1^{+0.8}_{-0.3}$	0.64	$19.7^{+4.2}_{-3.5}$
*Suzaku*701028020	< 12.2	$1.78^{+1.23}_{-0.26}$	$1.65^{+0.21}_{-0.18}$	0.92/464	$8.1^{+2.1}_{-0.0}$	$5.5^{+1.3}_{-0.6}$	0.68	$15.4^{+2.8}_{-2.4}$
*Suzaku*701028030	< 6.2	$1.49^{+0.28}_{-0.16}$	$1.41^{+0.69}_{-0.32}$	0.82/331	$7.7^{+0.4}_{-0.1}$	$2.1^{+0.4}_{-0.2}$	0.27	$13.1^{+11.2}_{-4.9}$
*Swift*28003	$0.8^{+62.7}_{-0.8}$	4.51(> 2.08)	$1.46^{+0.27}_{-0.3}$	1.13/33	9.8			$23.4^{+20.9}_{-6.1}$

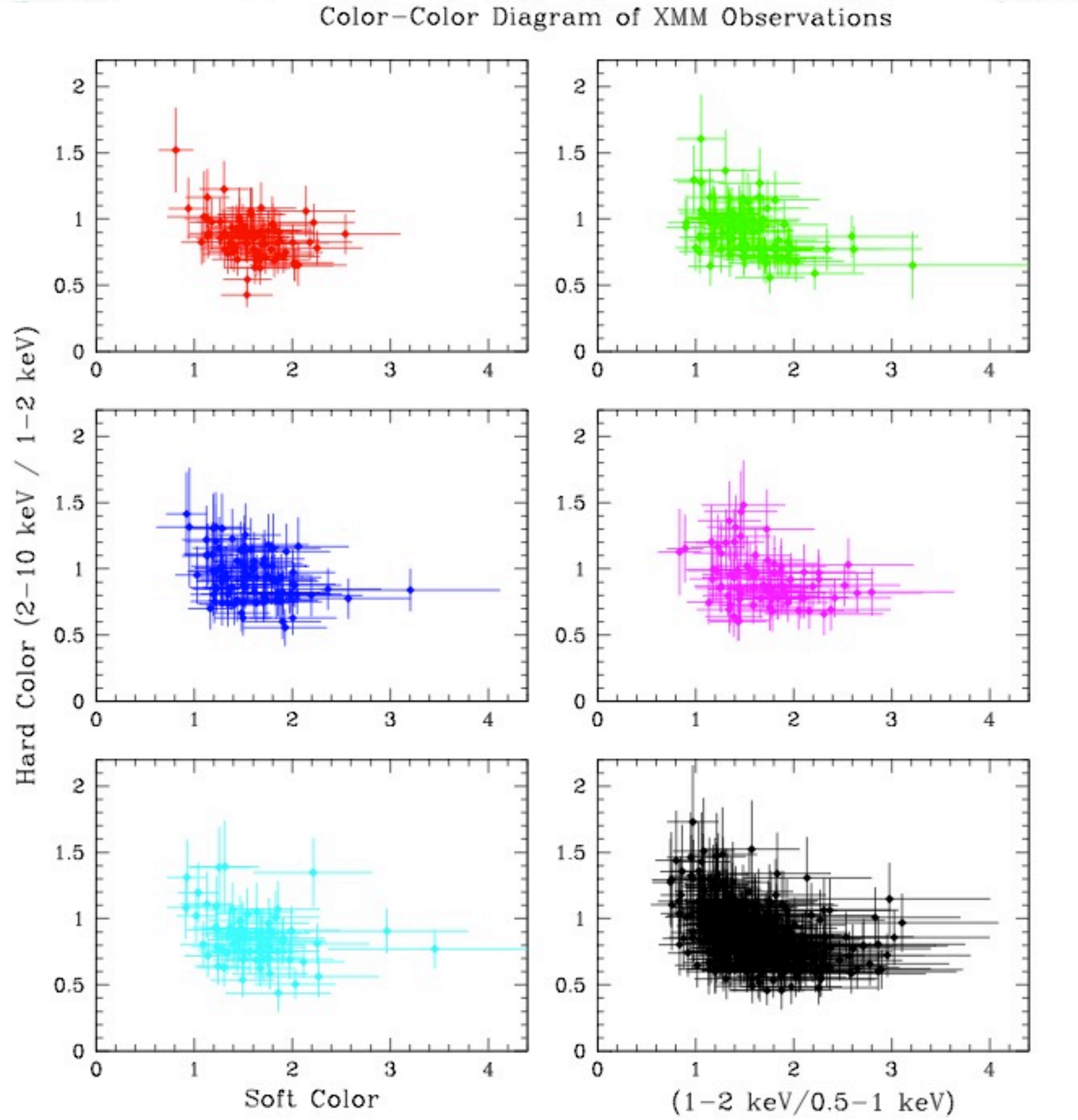

Color–Color Diagram of XMM Observations
Hard Color (2–10 keV / 1–2 keV)
Soft Color
(1–2 keV/0.5–1 keV)

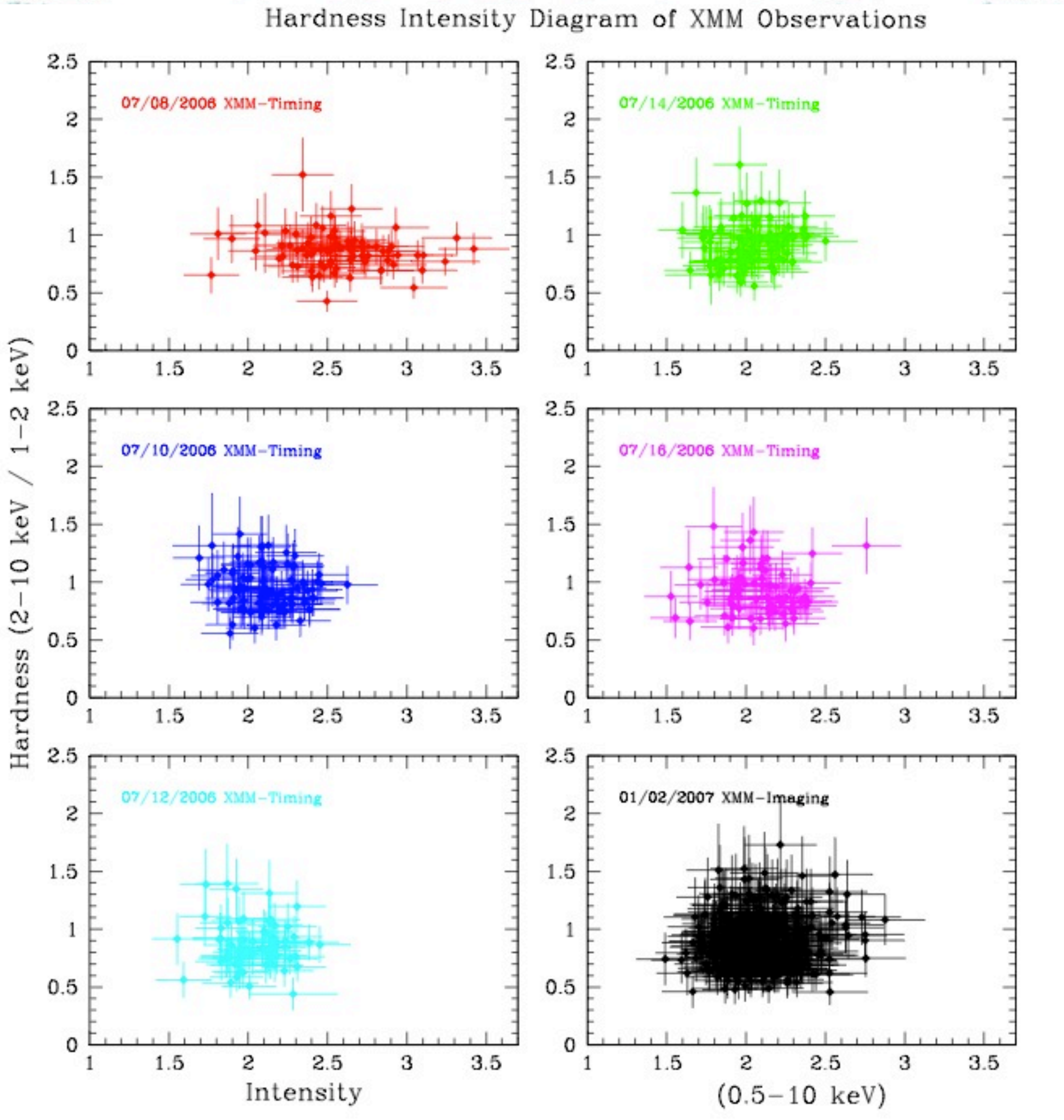

Hardness Intensity Diagram of XMM Observations
07/08/2006 XMM-Timing
07/14/2006 XMM-Timing
07/10/2006 XMM-Timing
07/16/2006 XMM-Timing
07/12/2006 XMM-Timing
01/02/2007 XMM-Imaging
Hardness (2-10 keV / 1-2 keV)
Intensity
(0.5-10 keV)

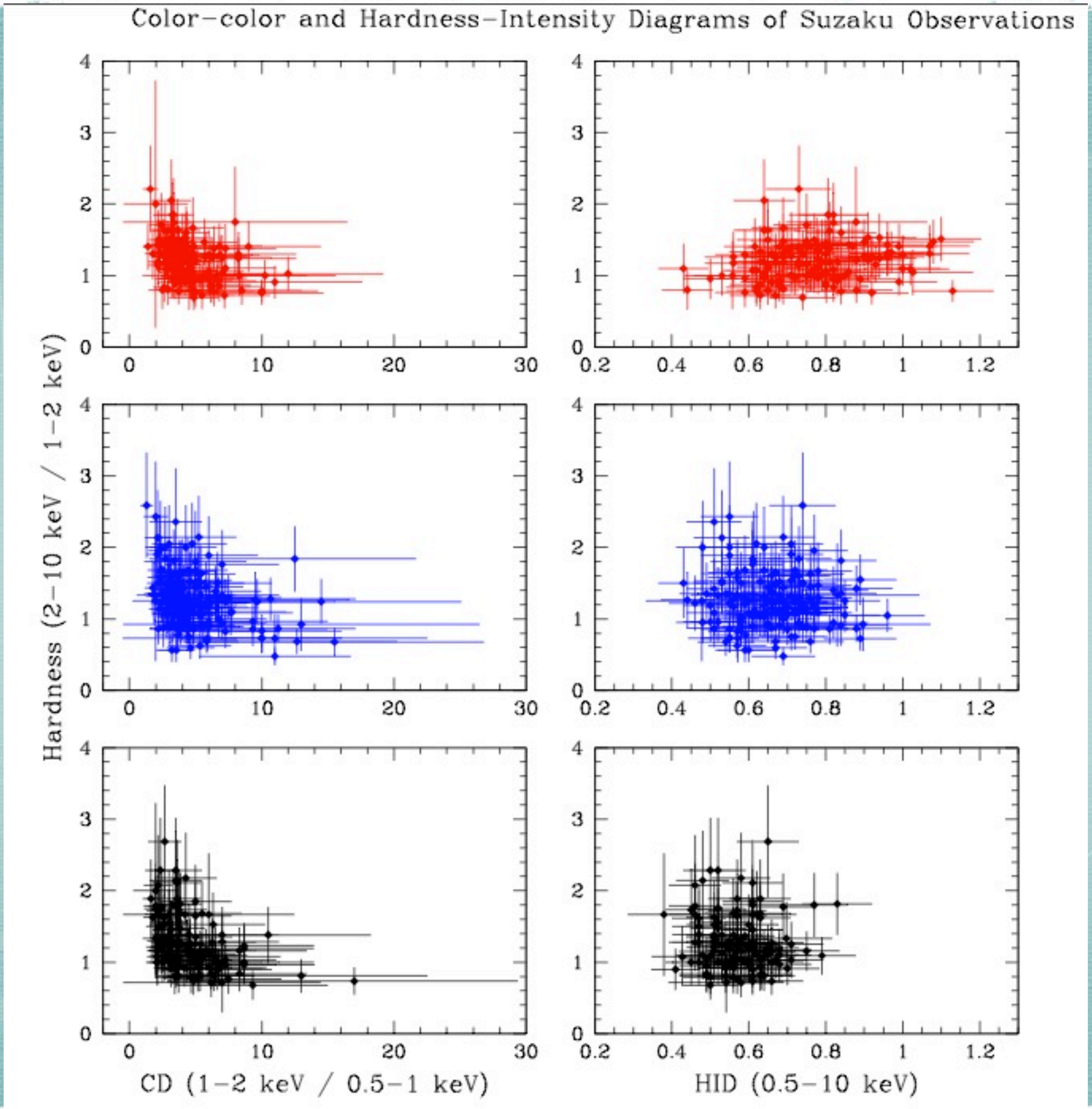

Color-color and Hardness-Intensity Diagrams of Suzaku Observations
Hardness (2-10 keV / 1-2 keV)
CD (1-2 keV / 0.5-1 keV)
HID (0.5-10 keV)

Summary

- The high luminosity is unlikely due to the superposition of multi-sources. Even if Bo375 contains more than one source, there at least one which dominates most of the energy output.
- Relativistic beaming is unlikely, because of the persistent source brightness and less of variability. However, anisotropic beaming due to the strong outflow or corona might be possible.
- It might be a neutron star accretes in a very unique way which produces persistent high luminosity.
- It might be a black hole with a much smaller mass than we usually found in our own Galaxy. (3~4 Msolar)

Holmberg IX X-1 in different luminosity states

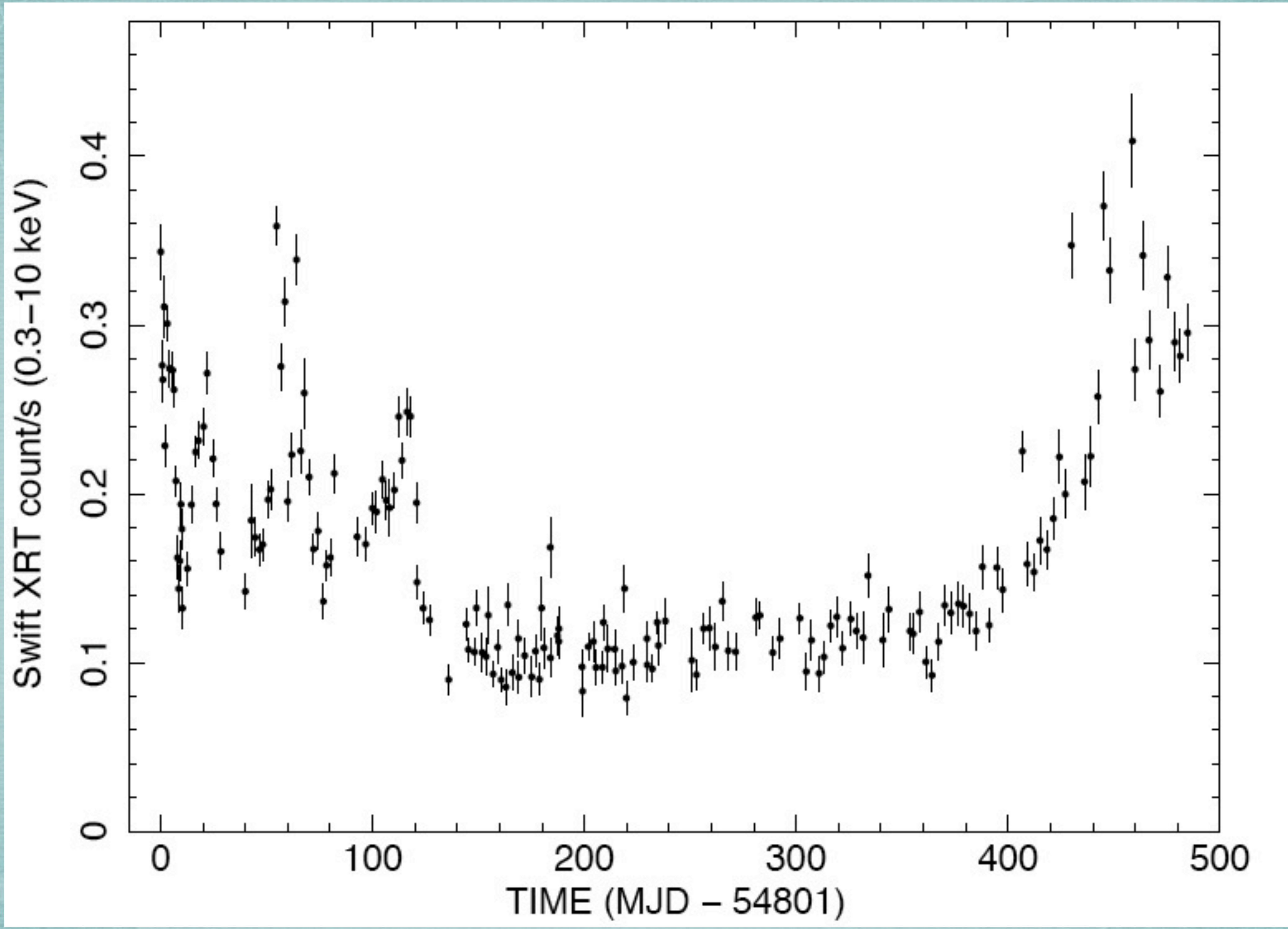

Swift XRT 0.3-10 keV lightcurve of Holmberg IX X-1 between 2008 December. 1 and 2010 March 31.

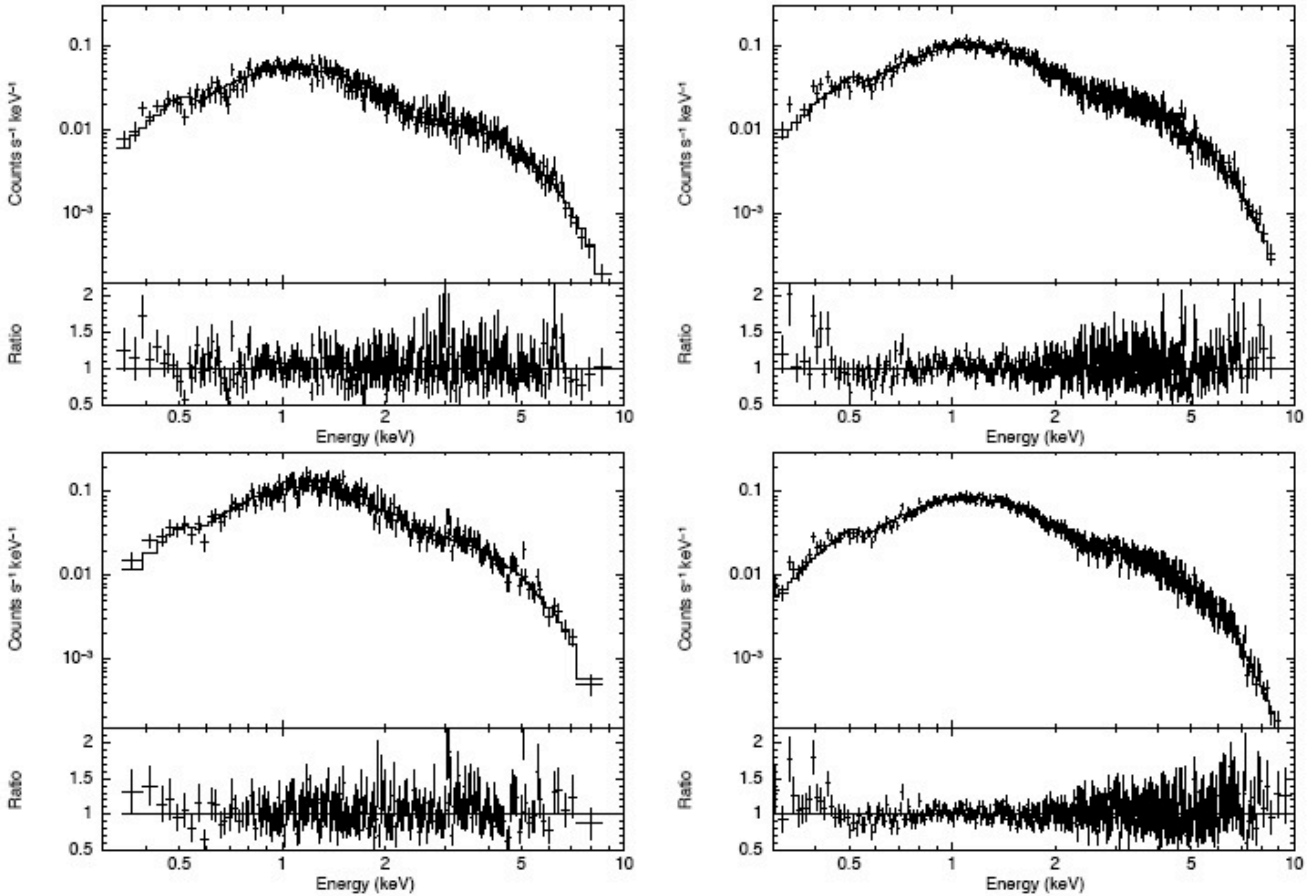

Swift XRT 0.3-10 keV spectra taken during the "low" state (upper left), "variable" state (upper right), "high" state (lower left), and all data (lower right). All spectra can be well described by a dual thermal model with a black body temperature of ~0.2 keV and a MCD temperature of ~ 2 keV.

Model parameter	Low state	Variable state	High state	All data
Power-law model				
N_H (10^{21} cm^{-2})	1.74 ± 0.13	2.16 ± 0.10	2.96 ± 0.23	2.16 ± 0.07
Γ	1.74 ± 0.04	1.86 ± 0.03	2.00 ± 0.06	1.86 ± 0.02
χ^2/dof	430.6/315	537.5/445	238.2/220	786.7/535
$L_{0.5-10}$ (10^{40} erg s^{-1})	1.00	1.66	2.48	1.58
MCD + Power-law model				
N_H (10^{21} cm^{-2})	$2.60^{+0.64}_{-0.51}$	$2.80^{+0.63}_{-0.51}$	$4.12^{+1.50}_{-1.28}$	$3.16^{+0.53}_{-0.44}$
Γ	1.68 ± 0.06	$2.65^{+0.53}_{-0.48}$	3.47 ± 1.03	$3.02^{+0.41}_{-0.37}$
kT_{in} (keV)	$0.20^{+0.06}_{-0.05}$	$2.25^{+0.23}_{-0.18}$	$1.69^{+0.18}_{-0.15}$	$2.11^{+0.12}_{-0.11}$
Norm	71^{+206}_{-55}	$0.012^{+0.007}_{-0.006}$	$0.061^{+0.038}_{-0.027}$	$0.016^{+0.005}_{-0.004}$
χ^2/dof	410.8/313	515.7/443	205.7/218	695.4/533
$F_{MCD}/F_{Total}{}^a$	0.13	0.46	0.50	0.52
$L_{0.5-10}$ (10^{40} erg s^{-1})	1.15	1.75	3.02	1.78
MCD + Blackbody model				
N_H (10^{21} cm^{-2})	$1.39^{+0.16}_{-0.18}$	1.20 ± 0.10	$1.56^{+0.40}_{-0.29}$	$1.25^{+0.11}_{-0.09}$
kT (keV)	$0.22^{+0.02}_{-0.12}$	0.26 ± 0.01	0.26 ± 0.04	0.25 ± 0.01
kT_{in} (keV)	$2.05^{+0.12}_{-0.10}$	1.86 ± 0.05	$1.60^{+0.10}_{-0.03}$	1.84 ± 0.06
Norm	$0.014^{+0.001}_{-0.003}$	0.037 ± 0.004	$0.086^{+0.028}_{-0.023}$	0.033 ± 0.004
χ^2/dof	348.2/313	489.7/443	203.7/218	625.3/533
$F_{MCD}/F_{Total}{}^a$	0.85	0.85	0.86	0.85
$L_{0.5-10}$ (10^{40} erg s^{-1})	0.88	1.38	2.0	1.35
DISKPN + EQPAIR model				
N_H (10^{21} cm^{-2})	2.22 ± 0.25	$1.92^{+0.21}_{-0.09}$	$2.26^{+0.38}_{-0.36}$	$2.01^{+0.10}_{-0.23}$
T_{max} (keV)	$0.26^{+0.06}_{-0.01}$	0.28 ± 0.02	$0.31^{+0.11}_{-0.06}$	0.29 ± 0.02
$l_h/l_s{}^b$	$5.41^{0.51}_{-0.25}$	3.27 ± 0.13	$3.05^{+1.06}_{-0.88}$	$3.89^{+0.10}_{-0.14}$
τ	$26.66^{+2.03}_{-1.49}$	19.45 ± 1.18	23.74 ± 6.24	$23.77^{+0.91}_{-0.99}$
χ^2/dof	354.8/312	496.7/442	203.9/217	643.9/532
$L_{0.5-10}$ (10^{40} erg s^{-1})	1.03	1.72	2.17	1.47

Optical counterparts of ULXs in the BCD galaxy NGC4861

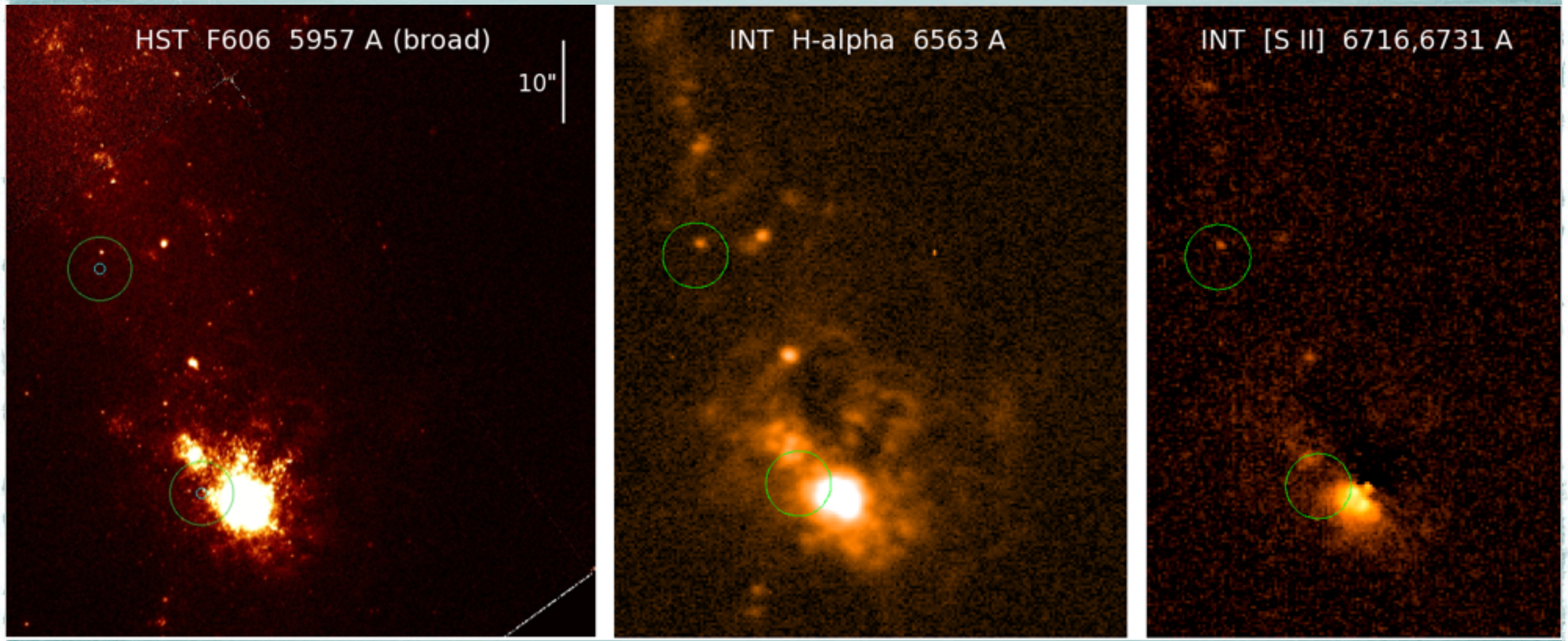

Chandra proposal for better astrometry has been approved.
More optical observations will be requested.

About PSR J1023+0038

PSR J1023+0038 was identified as a LMXB in 2006 (Homer et al.)

The radio MSP was found subsequently (Archibald et al. 2009)

The disk clearly showed an accretion disk before 2002 (Wang et al. 2009)

The disk has disappeared afterward (Archibald et al 2009)

Radio Pulsation was found in 2007 (Archibald et al 2009)

X-ray orbital period and pulsation found (Archibald et al. 2010 and this work)

Gamma ray emission from Fermi found (this work 2010)

Gamma-ray emission from PSR J1023+0038

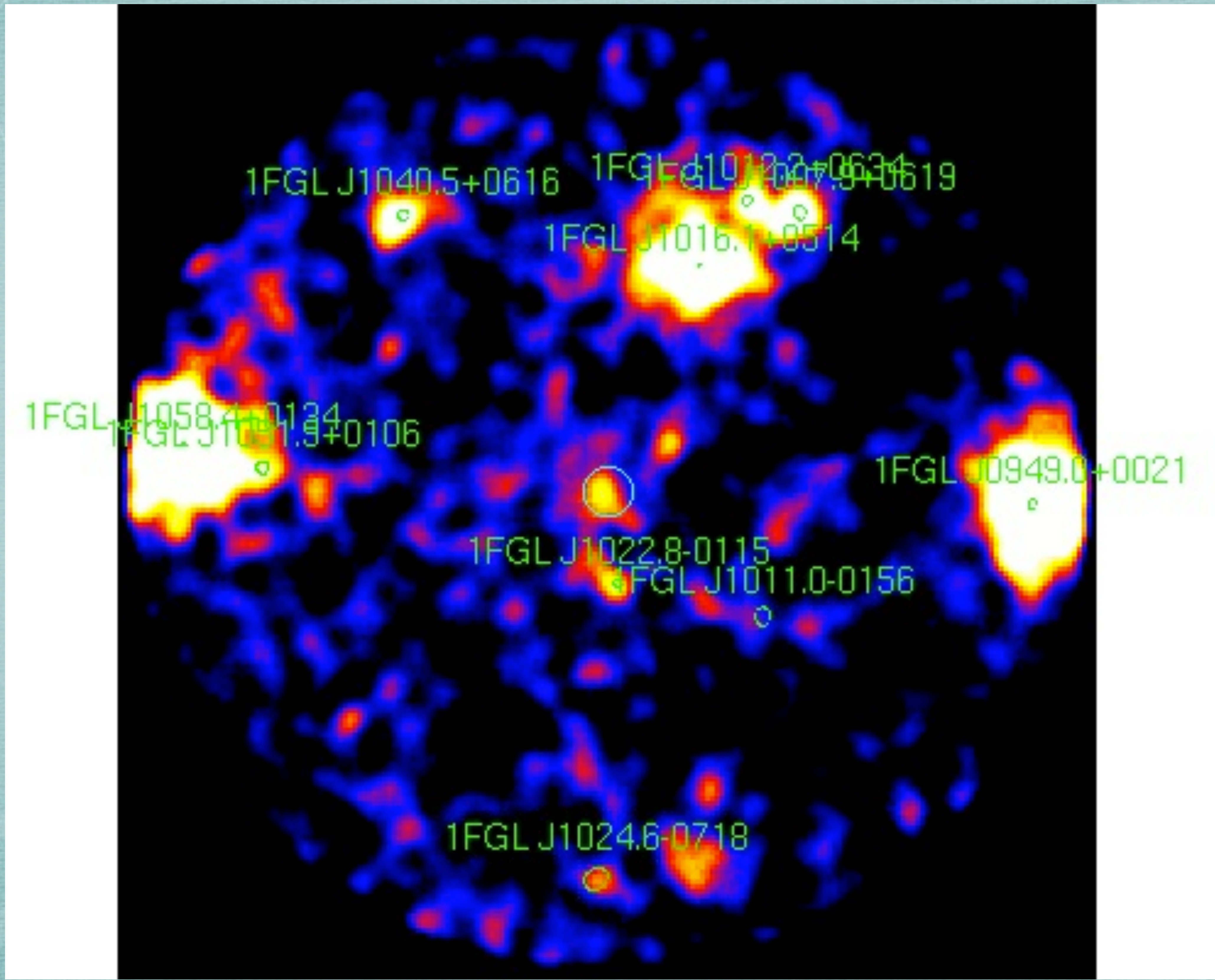

TS map of PSR J1023+0038

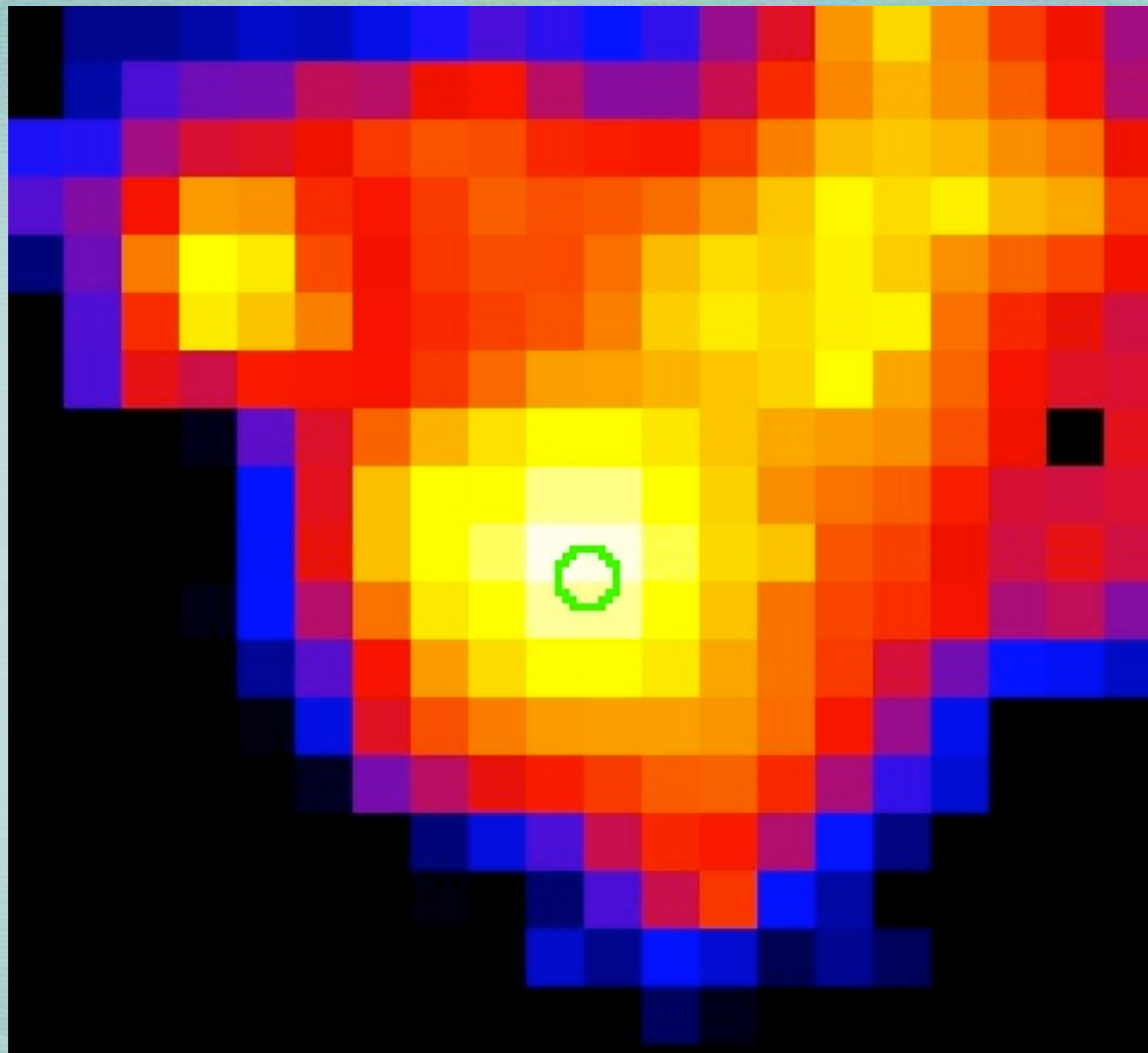

With TS value ~54 which corresponds to ~ 7 sigma significance.

Spectral parameter values of γ-ray emission from J1023.

Model[a]	Photon flux[b] (>200 MeV) (photons cm^{-2} s^{-1})	Energy flux (>200 MeV) (erg cm^{-2} s^{-1})	Photon Index Γ_γ	Cutoff energy (MeV)	γ-ray luminosity[c] (>200 MeV) (erg s^{-1})
PL	$8.2^{+1.5}_{-1.5} \times 10^{-9}$	$5.4^{+3.0}_{-3.5} \times 10^{-12}$	2.9 ± 0.2	—	$1.1^{+0.6}_{-0.7} \times 10^{33}$
PLE	$7.6^{+6.6}_{-4.2} \times 10^{-9}$	$4.9^{+6.1}_{-3.0} \times 10^{-12}$	1.9 ± 0.3	700 ± 230	$9.9^{+12.4}_{-6.1} \times 10^{32}$

[a] PL=power law model; PLE=power law with an exponential cut-off model
[b] All the quoted errors are statistical and 1σ for one parameter of interest.
[c] The pulsar distance is taken as 1.3 kpc.

Gamma ray power is low compare to the spin-down power of the pulsar. Also the spectral photon index is quite steep compare to the typical Gamma ray pulsars found previously.

This is probably due to the viewing angle.

Future Work

Continuously working on current research, building up skill for multi-wavelengths observations.

&

Most importantly, hopefully Lofar will be able to find radio transients very soon!